WFC3 Instrument Science Report 2010-07

First On-orbit Measurements of the WFC3-IR Count-rate Non-Linearity

A. G. Riess
March 10, 2010

ABSTRACT

Previous HgCdTe detectors on HST have suffered from a count-rate dependent non-linearity, motivating an investigation of a similar effect on the WFC3-IR detector. An initial measurement of this effect was made by comparing the photometry of star clusters observed over a wide dynamic range and at overlapping wavelengths in WFC3-IR and NICMOS and/or ACS-WFC. Utilizing a color term to account for differences in the observed bandpasses, we find a significant detection of a non-linearity in WFC3-IR photometry which is in the same direction but a few times smaller than that of NICMOS. From 235 stars in 47Tuc observed with WFC3-IR in F110W and F160W and in similar bandpasses in NICMOS Camera 2, we measure a non-linearity of WFC3-IR of 0.011+/-0.0023 and 0.010+/-0.0025 mag per dex, respectively, over a range of 10 magnitudes (4 dex). An independent measurement utilizes 1390 stars in NGC 3603 observed with ACS-WFC F850LP and WFC3-IR F098M and yields a very similar result, 0.010 +/- 0.0033 mag/dex. The consistency of this measurement from two different comparison detectors of different technology indicates this result is robust. The impact of this non-linearity is that photometry of faint (i.e., sky dominated) sources calibrated with WFC3-IR zeropoints will appear 0.04 +/-0.01 mag too faint.

Introduction

Experience with the HST NICMOS HgCdTe infrared detectors revealed a number of non-linearities associated with photon counting. The well-known non-linearity of detected counts with total incident flux (i.e., the signal non-linearity) is characterized by varying the integration time of a standard source, in the lab or on-orbit (Hilbert 2008) and calibrating its effect. Far more pernicious is a non-linearity with *count-rate*, also referred to as a failure of reciprocity or the "Bohlin Effect" (Bohlin, Linder, Riess 2005). While the mechanism of this type of non-linearity is not yet fully understood, it appears to result from charge trapping (Smith et al. 2007). Its presence has been well-established both in laboratory measurements of similar detector types as well as on-

orbit in a direct manner; through the measured difference between source and source plus background light. That the same sources vary (as a power law) in their apparent count rate in the presence of additional lamp light indicates that the critical detector parameter is the rate, not the integrated signal or signal history.

For NICMOS the size of the effect depended somewhat on the camera (which changes the pixel size and count rate) and filter (which changes the energy flux), ranging from a 6% to 10% loss in measured flux per factor of ten decrease in flux in F110W for Camera 2 and 1, respectively. The non-linearity diminishes toward the red, reaching 3% for Camera 2 for F160W. For typical, faint science sources (i.e., below the sky) the net effect can be quite large because photometry zeropoints are established with stars which are 10 magnitudes or 4 dex brighter. Thus the net effect on the faint end of science photometry (i.e., sky-dominated) in the blue is 0.2 to 0.4 mag when using the extrapolation from zeropoint calibration to the sky flux. The size of the effect was unchanged between Cycles 7 and 14 as seen in archival data taken with flat lamps on and off despite the 12 degree cooler running temperature in Cycle 14 (de Jong et al. 2006)

Because the count-rate non-linearity was not detected in NICMOS until late in the development cycle of WFC3, a similar lamp assembly with the ability to add flux to an external measurement was not employed in the WFC3 IR channel. However, we expect the size of the effect to be smaller for WFC3-IR based on the reduced level of persistence, a more visible result of charge trapping. To produce a varying count-rate on the WFC3 IR detectors we intend to observe a star cluster during cycle 17 under near-CVZ-like conditions, thus varing the incident sky flux accompanying stellar sources between the day and night side of the orbit (GO 11933).

An alternative approach to externally increasing the count-rate and comparing the result is to measure a sequence of stellar count-rates whose relative values have previously been independently determined. Because this method relies on both the reliability of the other detector as well as on corrections for the different parts of the observed spectral energy distributions (i.e., astrophysical knowledge), it is not as direct as the method of adding background light. If the comparisons are made with well-understood astronomical sources (e.g., stars) over similar wavelength ranges observed with well-characterized detectors, the results should provide valuable constraints. Even better would be to use more than one independent detector to verify the results. Here we use both ACS-WFC and NICMOS as independent calibrators for WFC3-IR of count-rate sequences in star clusters. NICMOS HgCdTe detectors can be corrected for their non-linearity over the relevant brightness range using the coefficients from de Jong et al. (2006) any apparent non-linearity remaining in the comparison should be due to WFC3-IR. For ACS-WFC, observations at the red end of its sensitivity fairly well match the blue end sensitivity of WFC3-IR. CCDs also have far superior linearity to HgCdTe detectors (Gilliland 2004) making this a valuable comparison. We use archival data to carry out this comparison.

Analysis

To meaure the count-rate dependence of WFC3-IR we assume the magnitude of a star in a WFC3-IR band, *x*, i.e., m_x, can be expressed as a transformation of the magnitude in an independent detector and passband, m_y and its color, m_y-m_z. To account for diffences in zeropoints and aperture corrections, we will reference all magnitudes to the same standard star, P330E, measured in the same sized aperture. Hence we define the following relation:

$\mathbf{m\_y_{star}}$-m_y_{p330e}=a_0*($\mathbf{m\_x_{star}}$-m_x_{p330e})+ a_1*[($\mathbf{m\_y_{star}}$-m_y_{p330e})-($\mathbf{m_z_{star}}$-m_z_{p330e})] (1)

where a_1 is a conventional color term and a_0 is the parameter of interest, i.e., the non-linearity between WFC3-IR and another detector. Bold face denotes an array of measurements and red type are terms relating to stellar color. Our asumed functional form of the non-linearity, is the same as de Jong et al. (2006), where the true count rate, cr=flux$^{\alpha}$ where α=2-a_0 . The color term, a_1, may be determined synthetically using the iraf package *synphot* in *stsdas* to empirically measure the color relation using model stellar SEDs or treated empirically as a nuisance parameter in a 2-parameter simultaneous fit for a_0 and a_1 in equation (1). We do both below, employing *synphot* to constrain the color term and then combine that constraint with the simultaneous fit to improve upon this estimate.

We use the following matrix format to compactly express equation (1), minimize the χ^2 statistic and determine the free parameters:

$$y=Lq \qquad (2)$$

$$\chi^2=(y-Lq)^T C^{-1}(y-Lq) \qquad (3)$$

where $\mathbf{y}$=[($\mathbf{m\_y_{star}}$-m_y_{p330e}) - a_1*[($\mathbf{m\_y_{star}}$-m_y_{p330e})-($\mathbf{m_z_{star}}$-m_z_{p330e})], 0] with a_1 and its uncertainty, σ_{a1}, estimated from *synphot*,

q=(a_0, Δa_1)

and

L is the matrix, L=

($\mathbf{m\_x_{star}}$-m_x_{p330e})	($\mathbf{m_y_{star}}$-m_y_{p330e})-($\mathbf{m_z_{star}}$-m_z_{p330e})
0	1

and C is the error matrix of the measurements. As we have already corrected the stellar magnitudes for the synphot-based estimate of the color term, a_1, the new parameter Δa_1 is the *delta* color correction determined from the data. While the first *n* linear equations (where *n*=# stars) follow from equation (1), the last entry in $\mathbf{y}$, the last row in L, and the last corner entry of C accommodate the simple relation, 0= $\Delta a_1 \pm \sigma_{a1}$ thus including the constraint on the color term from synphot. Including this term provides emprically for a perturbation to the color term if warranted

by the data and the final color term will be given by $a_1+\Delta a_1$.

The maximum likelihood estimate of q is given by $(L^TC^{-1}L^{)-1}L^TC^{-1}y$ with standard errors $(L^TC^{-1}L)^{-1}$ (Rybicki and Press 1992). With this formalism we now proceed to its application to WFC3-IR, ACS and NICMOS stellar magnitudes.

NICMOS, Camera 2 to WFC3-IR

We identified two archival NICMOS Camera 2 pointings of 47Tuc which overlap a field of WFC3-IR in the same filters. The fields are located 6' West of the core, one of which is shown in Figure 1.

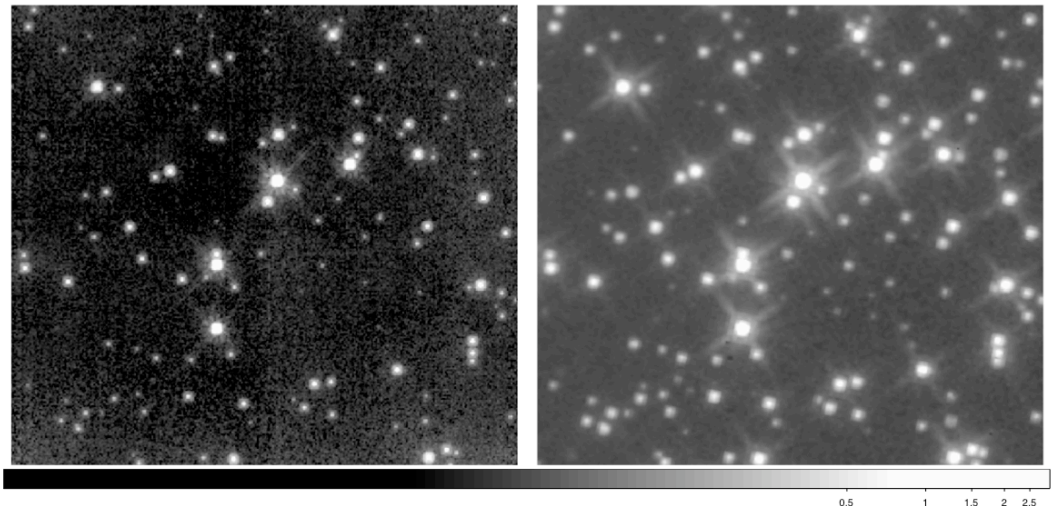

Figure 1: NIC2 field in 47Tuc F110W (left) and corresponding region in WFC3-IR F110W (right).

Table 1 gives the datasets employed.

Table 1: WFC3/IR				
Filter	Exposure time(sec)	Date	Target	Proposal ID
F110W	746.1	2009-07-17	47TUC	11453
F160W	1645.4	2009-07-17	47TUC	11453
F110W	1.8	2009-07-13	P330E	11451
F160W	1.8	2009-07-13	P330E	11451

NICMOS, Camera 2:				
Filter	Exposure time (sec)	Date	Target	Proposal ID
F110W	511.6	2004-10-27	47tuc_1	10015
F110W	575.4	2004-10-27	47tuc_2	10015
F160W	511.6	2004-10-27	47tuc_1	10015
F160W	575.4	2004-10-27	47tuc_2	10015

F110W 9.674496	2005-07-08	P330-E	10381
F160W 23.92448	2005-07-08	P330-E	10381

For NICMOS, the data was obtained from the archive, consisting of 8, 1 minute dithers processed through *calnica* in *stsdas* to produce *cal.fits files. We then used multidrizzle to produce a single, rectified image. The same was done for the standard star P330E and the observations of P330E were selected to be as close in time as possible to those of 47Tuc. For WFC3-IR, the datasets were obtained from the archive and processed through *calwfc3* to produce *flt.fits files. These were then combined in mutidrizzle as well using an up-to-date geometric distortion table. A geometric transformation between NICMOS and WFC3-IR observations of 47Tuc in the same filter was determined from ~100 of the brightest matched stars in the field with free parameters of scale, rotation, x and y shifts. The transformation was then used to identify 235 matching stars in the two cameras in the two fields. Aperture photometry with radii of 0.2" was measured for all stars relative to P330E. All stars were well-detected (signal-to-noise > 20) allowing us measure their individual centroids without a centering photometric bias (which may occur for signal-to-noise < 4). We estimated the color term, a_1, synthetically as described in the Appendix. The result was a determination of 0.14 ± 0.04 and -0.14 ± 0.04 (NICMOS minus WFC3-IR per magnitude of NICMOS F110-F160W) for F110W and F160W, respectively. The color terms reflect the extended red response of NICMOS in F160W which has a pivot wavelength 0.7 microns redder than WFC3 and the bluer effective wavelength for NICMOS F110W by 0.3 microns in the pivot (because the WFC3-IR response is flatter than NICMOS). The NICMOS magnitudes were corrected for the count-rate non-linearity using the results from de Jong et al. (2006).

Table 2: Comparisons WFC3 Filter	Transform	a_0	mag/dex	Δa_1	Mean Dispersion (mag)	stars
F160W	NIC2, F160W	0.996 +/- 0.0009	0.010 +/-0.0022	0.018 +/- 0.016	0.11	227
F110W	NIC2, F110W	0.996 +/- 0.0009	0.011 +/- 0.0022	0.003 +/- 0.013	0.11	213
F098M	ACS, F850lp	0.996 +/- 0.0012	0.011 +/- 0.0031	-0.065 +/- 0.003	0.09	1406

The fits are shown in Figure 2 and 3. An iterative 2.5 σ clipping (P > 99%) was used to reduce the influence of outliers in the tails. The resulting, delta color terms, Δa_1, are both consistent with zero with uncertainties of ~0.015 mag, indicating that the fits' empirical color term is consistent with *synphot* and of somewhat greater precision. Similar departures from linearity are detected (at ~5 σ confidence) for each filter, thus we see no evidence of a wavelength dependence at the present precision. The implied correction for background-limited WFC3-IR photometry (the sky begins to dominate the source counts ~10 magnitudes or 4 dex fainter than P330E) is 0.04 +/- 01 mag in the

sense that WFC3-IR magnitudes are brighter by this amount than measured using standard star zeropoints. The faintest stars in the fit are 10.5 magnitudes fainter than P330E (i.e., 23rd mag) but the quality of the fit is probably limited to about 9 magnitudes fainter, leaving little extrapolation of the fit down to the sky level.

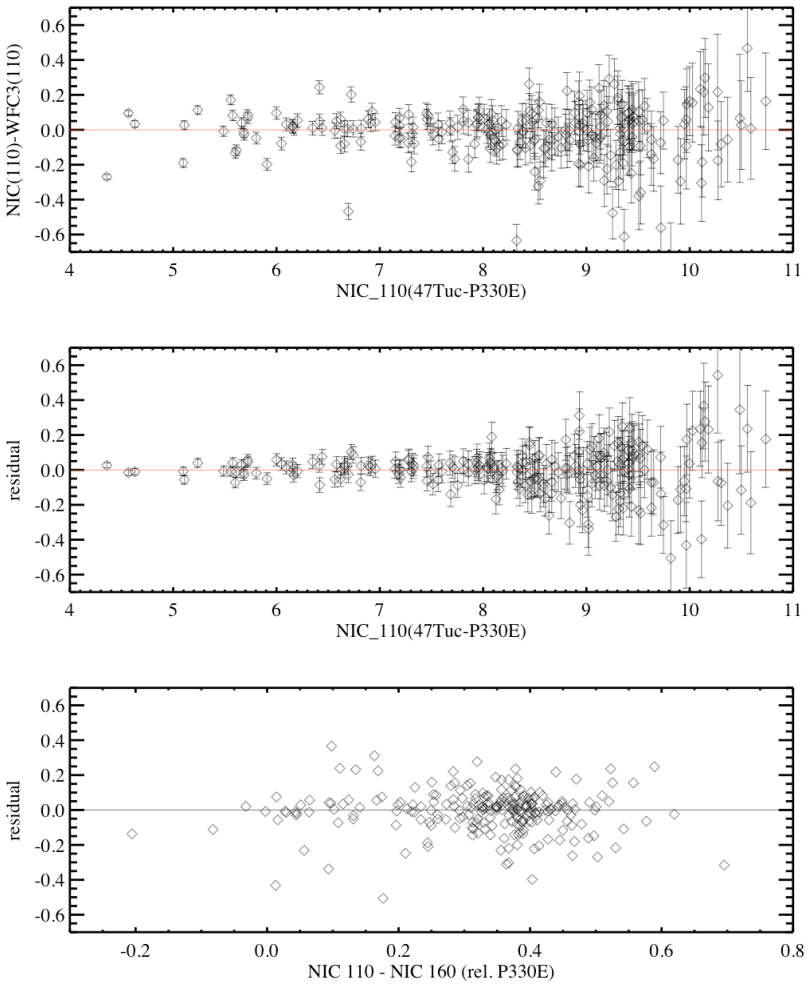

Figure 2: WFC3-IR F110W vs. NICMOS, Camera 2 F110W for 235 stars in 47Tuc. The upper panel shows the difference in photometry with both sets refenced to the same standard star, P330E. The middle panel shows the residuals from the transformation between the two sets, utilizing a color term and a non-linearity term. The bottom panel shows the residuals as a function of stellar color.

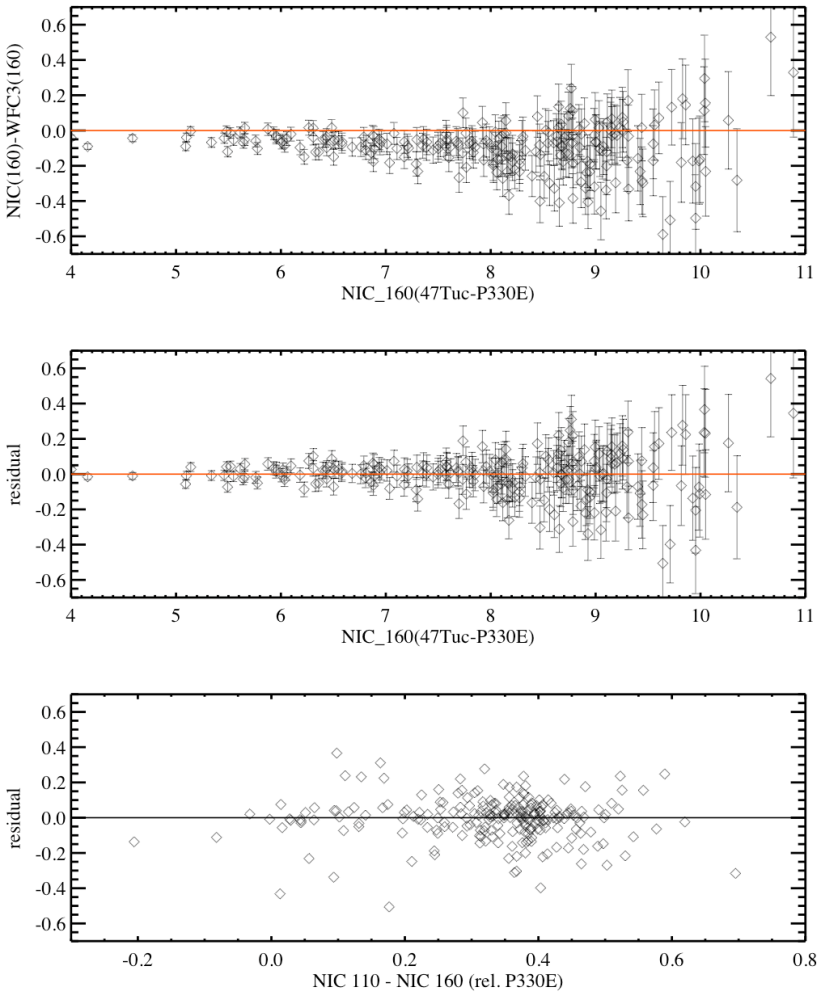

Figure 3: As Figure 2 but for F160W.

ACS-WFC to WFC3-IR

ACS-WFC F850lp provides the closest match to any WFC3-IR filter. Specifically F098M has about 50% overlap with F850lp in integrated throughput. The filter pivot wavelengths are 9030 A and 9860 A for F850lp and F098m, respectively. The difference between the F850lp and F098m is somewhat larger than between the filters of NICMOS and WFC3, but readily correctable with a color term determined for stars.

We identified observations of the open cluster NGC 3603 obtained in ACS-WFC3 F850lp (and F550m) as well as for WFC3-IR F098M. These are given in Table 3 and shown in Figure 4. These were retrieved from the archive and processed through multidrizzle as described before.

After registration, 1390 stars were identified at high significance (signal to noise > 20) between the matching frames. We did not include any stars redder than the M7 star VDB to avoid extrapolating our knowledge of the color relations (see Appendix). Photometry was initially measured with apertures of radius 0.24" and for ACS the photometry was corrected for imperfect CTE using the results of Chiamerge and Sirianni (2009). The color term determined from synphot was 0.10+/-0.03 for F850lp minus F098m per magnitude of color F550m-F850lp but this was revised in the fit by -0.06, indicating either somewhat better red response for ACS or blue response for WFC3-IR. The data for NGC 3603 had much better leverage on the color term than the NICMOS fit (or *synphot*) due to the large color range and quantity of stars. As shown in Figure 5, the residuals tighten considerably at a fixed brightness due purely to the color term.

The result for the WFC3-IR non-linearity is quite consistent with that derived from ACS as for NICMOS, yielding 0.013 +/- 0.0031 mag/dex (compared to F110W of 0.011 +/- 0.0023 mag/dex and F160W of 0.010 +/- 0.0025 mag/dex). As CCD's have far smaller non-linearities than IR detectors (ACS in particular; see Gilliland 2004), the independence of this result provides strong evidence that the measured non-linearities for WFC3-IR are robust.

A small tail of residuals in the fit is evident in the negative direction. These can be seen in the histogram of Figure 6 where this tail is seen to contain about 3% of the sample in excess of a normal distribution. Because these points also have errors which are 35% larger, they have very little of the total weight, about 1.5%, in the fit. The sense of these residuals is of these stars being fainter in WFC3-IR or brighter than ACS within the stellar aperture. These are likely from the latter as cosmic rays residuals remain in the ACS data which was composed from only 2 dithers. Future data sets would benefit with a greater number of cosmic ray splits, but the overall fit is little affected due to the low weight of these tails in the fit. As a test we repeated the fits reducing the stellar apertures to 0.16", a reduction in aperture area and included cosmic ray residuals of more than half. The result is 0.011 +/- 0.0029 mag/dex with a reduced dispersion from 0.10 mag to 0.08 mag. Indeed the population of the negative tail drops as seen in Figure 6 and Figure 7, but the overall affect on the non-linearity is modest and is not a simple function of the aperture radius (as seen by measuring at a third radius, r=0.2"). For consistency we chose an aperture for our final result in Table 2 and Figure 5 between these two, radius=0.2", which is the same as for the NICMOS comparison.

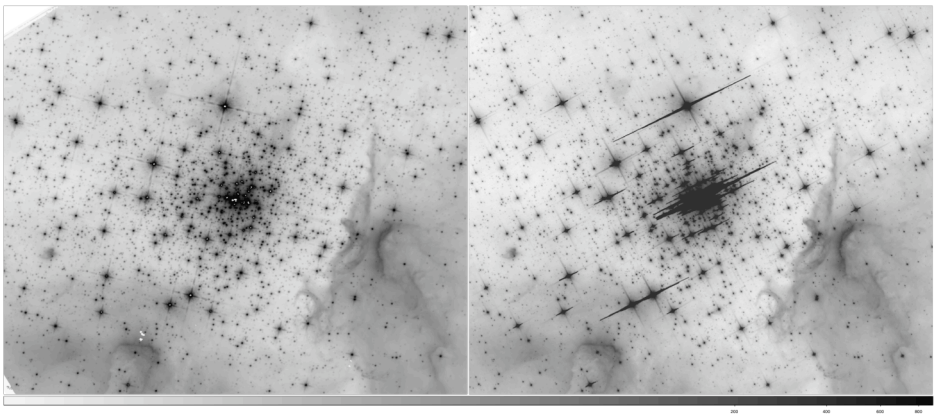

Figure 4: Field of NGC 3603

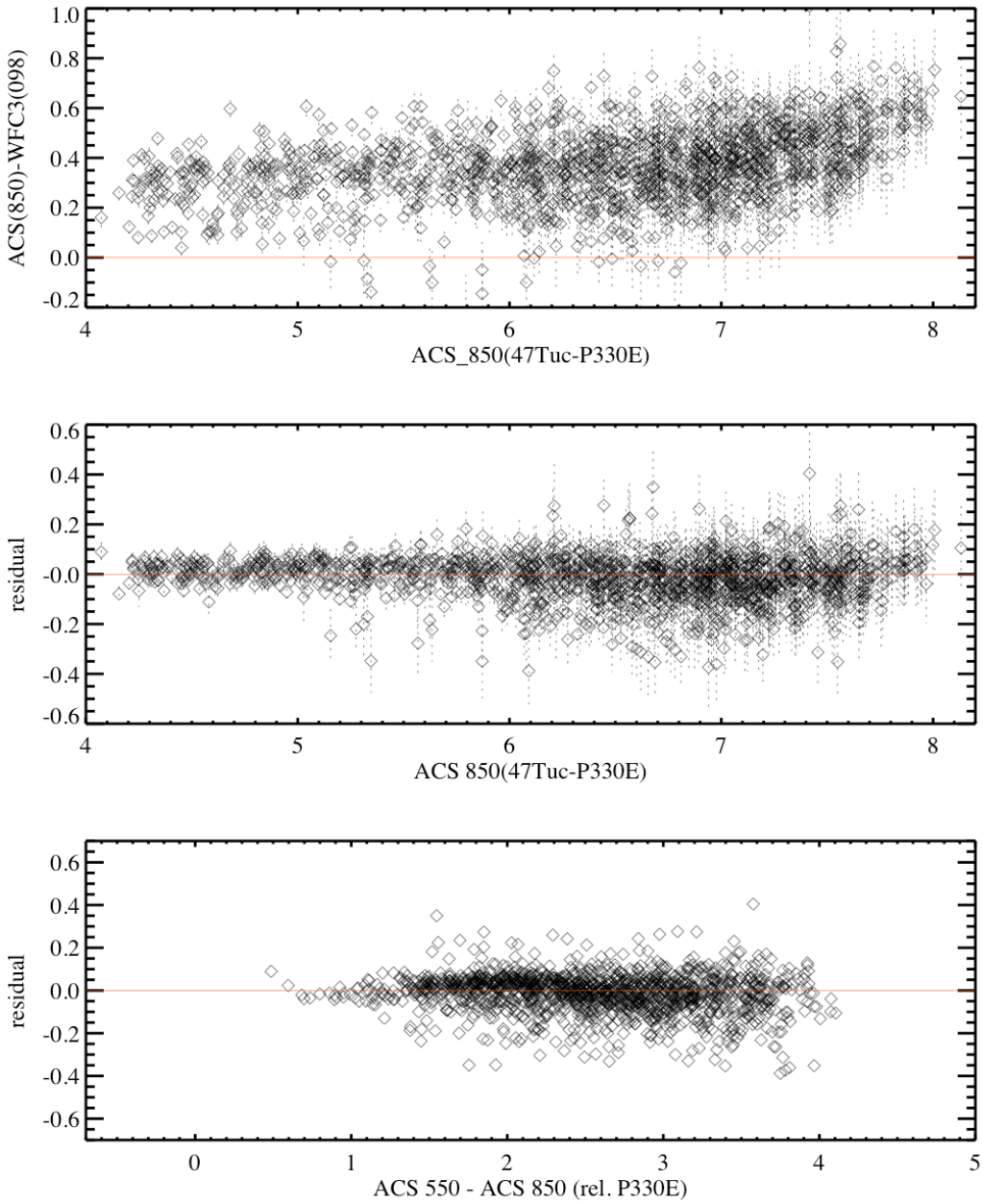

Figure 5: As Figure 2 but for WFC3-IR F098M vs. ACS-WFC F850LP

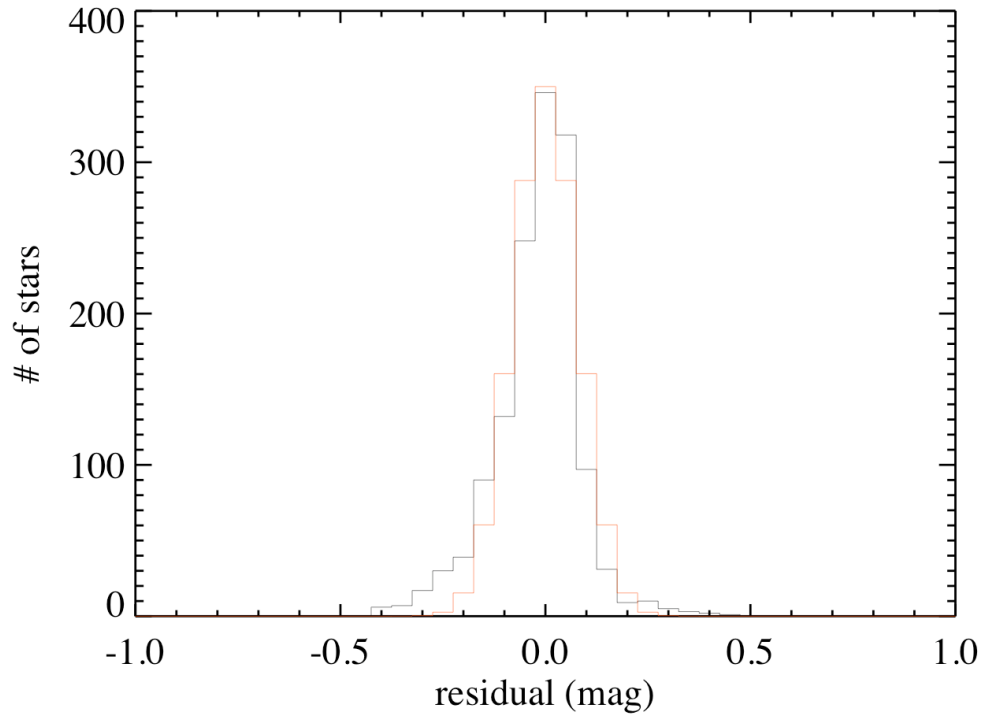

Figure 6: Histogram of residuals for WFC3-IR F098M vs. ACS-WFC F850LP with a photometry aperture radius of 0.24", compared to a gaussian with a dispersion of 0.08 mag. A small tail of negative residuals is apparent and likely arises from cosmic ray residuals in the ACS image (which was composed from only 2 dithers) but these have little affect on the fit.

Table 3: ACS-WFC				
Filter	Exposure time(sec)	Date	Target	Proposal ID
F850LP	6.0	2006-01-18	P330E	10374
F550M	678.0	2005-12-29	NGC3603	10602
F850LP	678.0	2005-12-29	NGC3603	10602
WFC3-IR				
F098M	3196.9	2009-08-27	NGC-3603	11360
F098M	1.8	2009-08-13	P330E	11451

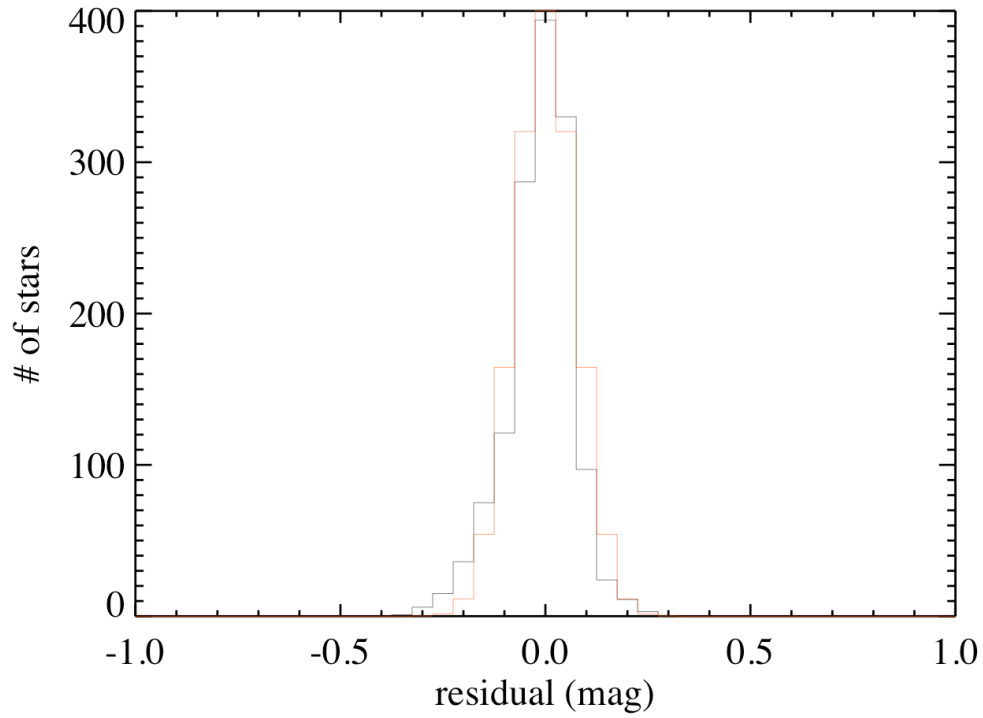

Figure 7: Same as Figure 6 but for r=0.16" sized aperture. The smaller aperture from Figure 6 reduces the impact of cosmic ray residuals in the ACS data and the negative tail, but overall has negligible affect on the fit.

Discussion

As non-linearity and persistence both appear to arise from the phenomenon of charge trapping (Smith et al. 2007, M. Regan, private communication), the former from the capture of charge and the latter from its release, it may be insightful to compare the relative persistence of WFC3-IR and NICMOS to compare to their relative non-linearity. In Figure 8 we show the level of persistence as a function of the prior illumination for WFC3-IR determined from the well-dithered observations of 47 Tuc. (The resemblance of the data to a Fermi-Dirac distribution probably relates to the occupation statistics of charge traps. In this case prior illumination controls the likelihood that traps are occupied, analogous to how the Fermi level determines the energy levels of electrons at a fixed temperature or in this case saturation level.) We can compare this persistence level to that seen in NICMOS (Figure 9), both shown after one e-fold of the decay of persistence after prior illumination. As seen, the overall persistence for WFC3-IR is less by a factor of 2 to 3 compared to NICMOS. Thus it appears that the trap density is lower for WFC3-IR than NICMOS by a factor of 2-3, an observation which also provides a basic test of the non-linearities presented in the previous section.

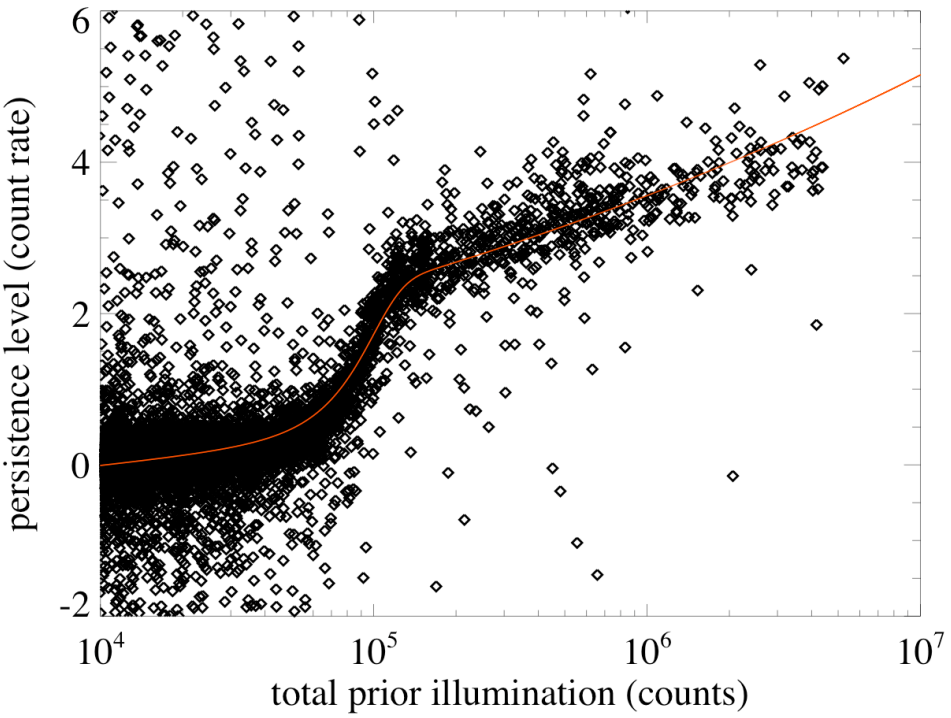

Figure 8: . WFC3-IR persistsnce level as a function of total prior illumination. A function characterizing the time decay of persistence (a double exponential as also used for NICMOS by Bergeron et al) was used to account for a small decay of persistence, a factor of 1.33, during the 76 seconds between exposures. The function in red is of the form of a Fermi-Dirac distribution $(e^{-cts/sat}+1)^{-1}$ where cts is prior illumination in counts and sat is the saturation of in counts of the pixel. Presumably the process motivating this function is that the prior illumination determines the likelihood that a trap is occupied.

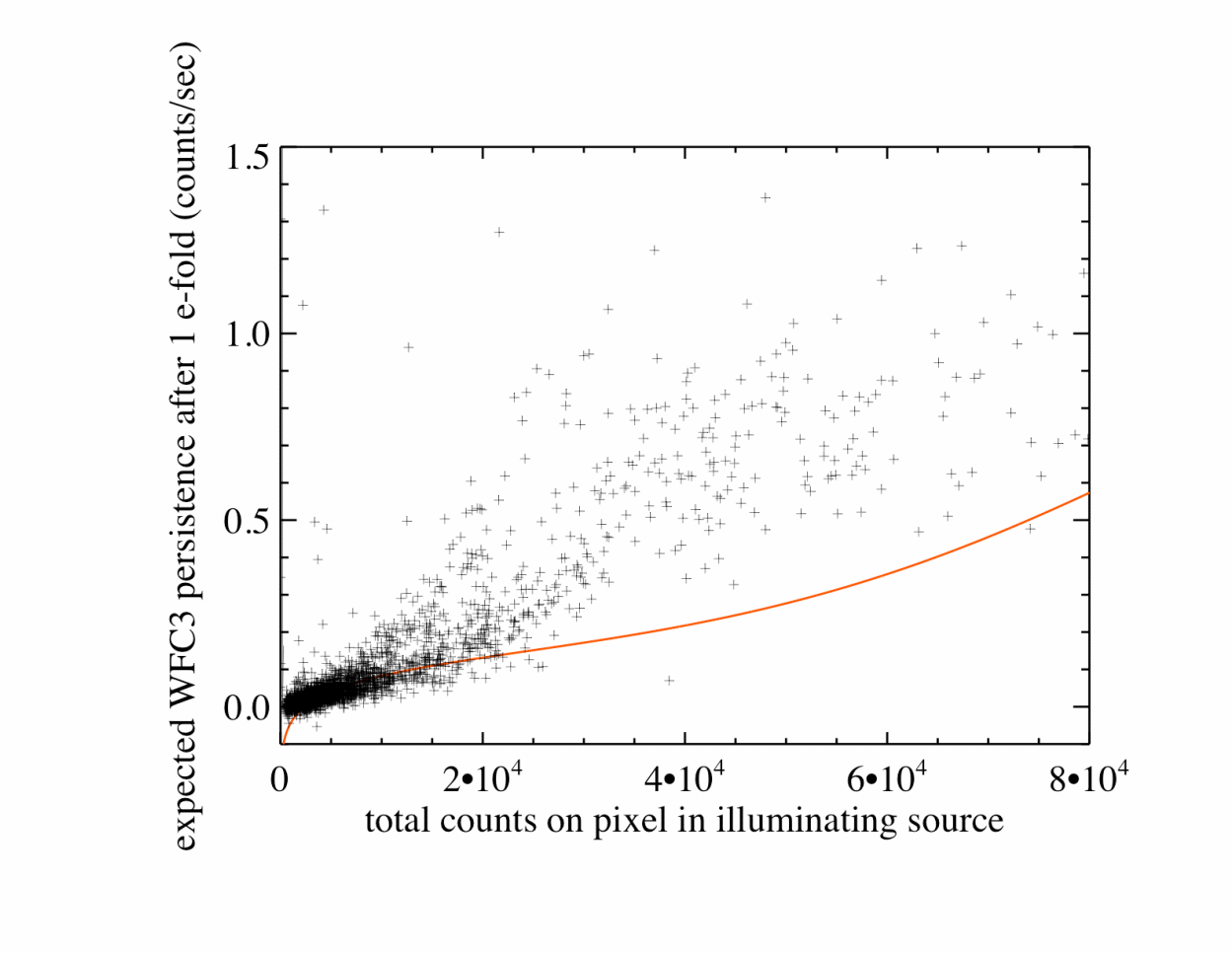

Figure 9: Persistence versus prior illumination observed for NICMOS (black crosses) compared to that determined for WFC3-IR (red line), each after an e-fold of persistence decay. As seen, the level of persistence is a factor of 2-3 greater for NICMOS than for WFC3-IR, which agrees with their relative ratio of non-linearity.

Conclusions

By comparing star cluster photometry between WFC3-IR, NICMOS Camera 2, and ACS-WFC we find a consistent value of non-linearity of 0.010 +/- 0.0025 mag/dex which is independent of wavelength at the present measurement precision. Future tests of this effect will be made in a more direct manner, by comparing the photometry of a star cluster with and without the presence of background light from the bright Earth limb. It is quite likely that the non-linearity we find is indeed dependent on count-rate as it is in the same direction as that found in NICMOS and a factor of a few smaller, both results expected from laboratory tests. However, future tests are important to better relate the effect to the conditions of the observation. The present calibration suggests that faint photometry measured at or below the sky level (i.e., 4 dex fainter than the standard star P330E used to set the WFC3-IR zeropoint) should be corrected 0.04 +/- 0.01 mag brighter to account for this non-linearity.

Acknowledgments

We express thanks to members of the WFC3 Team at STScI and Goddard for helpful discussions as well as Mike Regan and Eddie Bergeron at STScI. Additional thanks to Susana Deustua for reviewing this document.

Appendix:

Color Terms derived from synphot

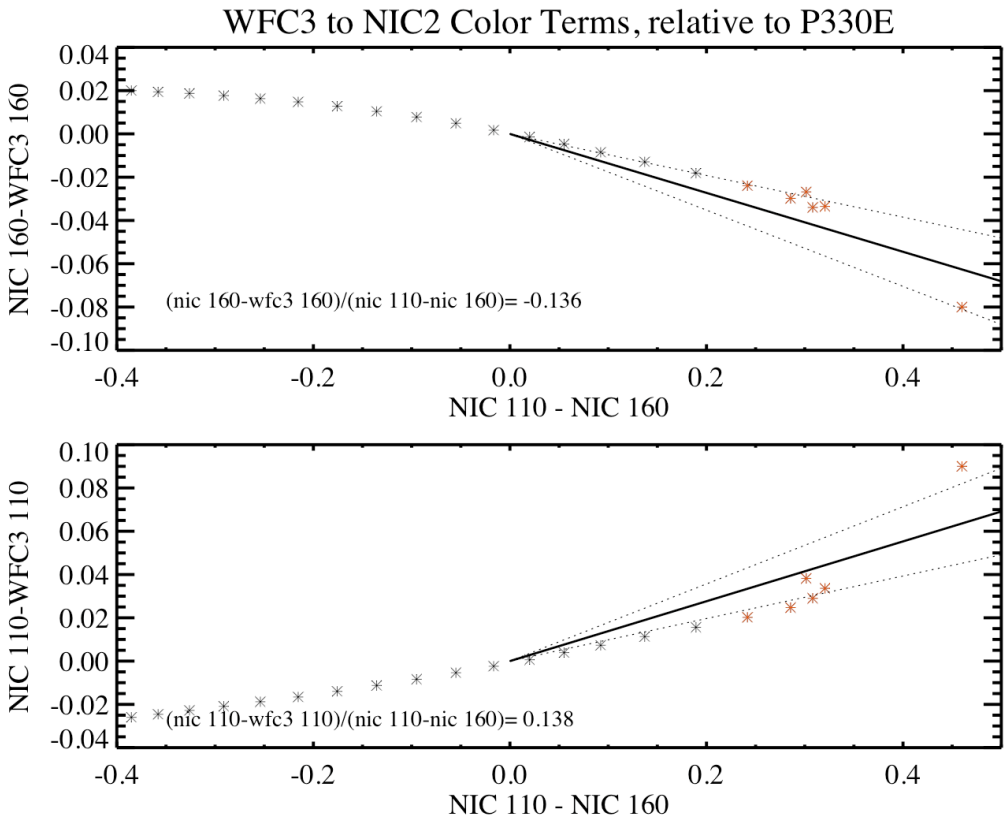

Figure A1. Synthetic color terms for NICMOS F110W and F160W versus WFC3 F110W and F160W.

In this appendix we show the synthetic determination of the color terms which provides the first estimate before a subsequent, empirical determination of a delta color term.

We use the sequence of Castelli and Kurucz (2004) stellar models to determine the synthetic color terms. The models, available in the iraf library *stsdas.synphot.calcspec,* include temperatures down to T=3500 degrees and we used those suitable for metal poor (Z=-0.2), main sequence

(gravity=g50) stars. We augmented this set with the addition of a very late type spectro-photometric standard star (VD8, an M7 dwarf) to extend the cool, red range of the calibration. The synthetic photometry was calculated using the iraf package *stsdas.synphot.calcphot* which includes the throughput of the telescope optics, instrument and filters. The color term is the magnitude difference between WFC3 and NICMOS (or ACS) divided by the color (NICMOS or ACS) of the stars. The fit (solid line) and estimated uncertainty of 0.04 (dotted line) is made to the color range relevant for the 47Tuc stars shown by the red points. A delta color term representing a correction to the synthetic value is determined from the empirical data as the term $\mathbf{\Delta a_1}$ in equation 1.

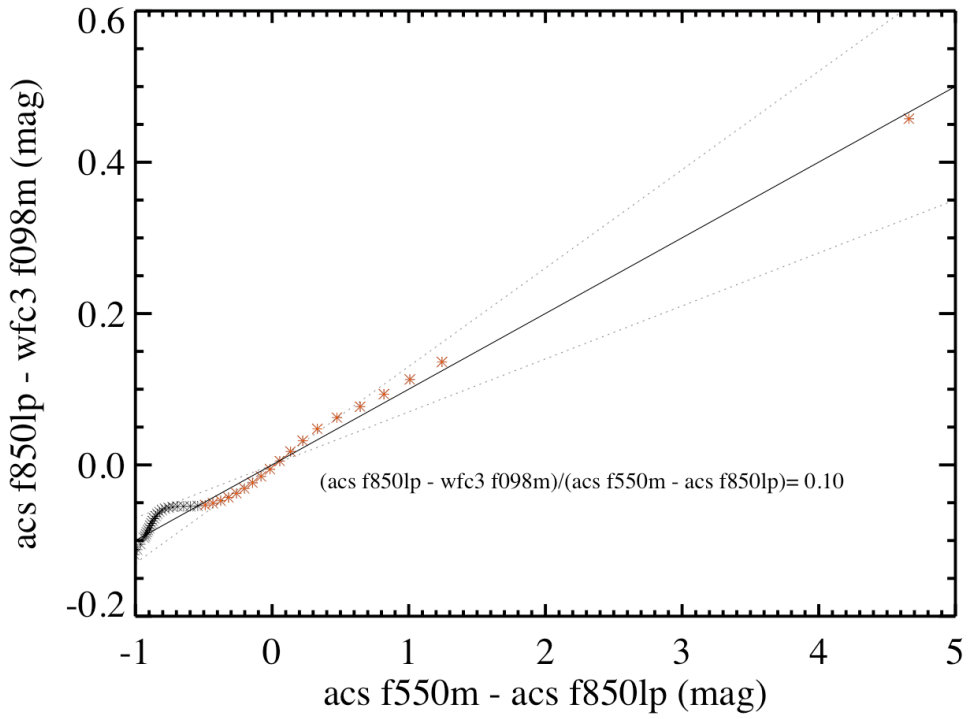

Figure A2: Same as Figure A1 but for ACS F850lp vs. WFC3 F098m.

References

Bohlin, R., Lindler, D., and Riess, A, 2005, NICMOS ISR 2005-002, "Grism Sensitivities and Apparent Non-linearity"

De Jong, R., Bergeron, E., Riess, A, Bohlin, R. 2006, NICMOS ISR 2006-001, "NICMOS count-rate dependent non-linearity tests using flatfield lamps"

Gilliland, R., 2004, ACS ISR 2004-01, "ACS CCD Gains, Full Well Depths, and Linearity up to and Beyond Saturation"

Hilbert, B, 2008, WFC3 ISR 2008-39, "WFC3 TV3: Testing: IR Channel Nonlinearity correction"
Smith, R., Zavodny, M., Bonati, M. and Rahmer, G., 2007, SPIE NSS2007, "Image Persistence in 1.7 micron cut-off HgCdTe Focal Plane Arrays for SNAP"